FLIGHT CONTROLLER DESIGN VIA A NEW METHOD TO ESTIMATE WORKLOAD LEVELS

Eri Itoh
Research Fellow of the Japan Society for the Promotion of Science,
Department of Aeronautics and Astronautics, The University of Tokyo,
7-3-1 Hongo, Bunkyo-ku, Tokyo, Japan

Keywords: *workload, pilot model, manual control, human-friendly operation, controller design*

Abstract

This paper is concerned with flight controller design which ensures human-friendly operation through a new method to estimate workload levels. This research carried out manual control experiments which are analogous to longitudinal dynamics of aircraft in the effect of disturbance input. Based on control theory, high-order and two-block pilot models are identified from experimental data. It is revealed that there is a strong relation between the pilot models and the corresponding workload comments. By making use of this strong relation, a new method was proposed to estimate workload levels for an application at a conceptual design stage. The proposed method allows us to design flight controller to assumed workload levels. Finally, the effectiveness of the designed flight controller is confirmed by demonstration experiments.

1 Introduction

Whenever human beings and mechanical systems work together, the overall performance depends on how well both the machine and the human beings do their jobs. Especially in aircraft, since the difficulty of operation may cause fatal incidents, equipped controller design needs to accomplish human-friendly systems. In flight controller design, two processes are needed. The primary stage is to propose a method to estimate the difficulty of pilot operation, while the secondary stage is to design a flight controller which guarantees practicable pilot operation by using the proposed method.

The present research defines a workload level as a degree of difficulty of human operation. Workload means both the physical and the mental load sustained by pilots in the course of carrying out tasks in order to achieve desired objectives. As pointed out in [1][2], there exist some workload estimation methods. For example, the physiological response of pilots[3], a degree of achieved performance[4], subjective ratings estimated by pilots[5], and the operator's ability to perform tasks[6][7]. Since these methods use the results of human operation, it is difficult to utilize at a conceptual design stage. References [4] and [5] estimate workload in conjunction with performance achievement, however this research tries to consider workload as an independent measure. With this background in mind, this paper proposes a new method which mathematically estimates workload levels through pilot models. These models are equational representations of the principles of human operations, and described as transfer functions in this paper. From the 1950's to the 70's, there was a large body of research which considered pilot models as low-order transfer functions [4], [8]-[19]. Recent high-performance vehicles that are equipped with advanced mechanical or electrical systems impose difficult operations on their pilots, and such operations are described as high-order transfer functions. Today, developments of computer techniques and methods of numerical analysis enable us to analyze high-order transfer functions and thus design systems which use them. Accordingly, this research adopts high-order pilot models that are based on transfer functions which are developed from experimental operation data. In addition, it may be noted that the pilot models provided in this paper are two-block models. How two-block models are used is considered in detail. High-order and two-block pilot models contribute to represent human operations on tracking tasks.

In this paper, firstly, a series of manual control experiments is described. These experiments are analogous to longitudinal dynamics of aircraft in the effect of disturbance input. Experimental data was collected together with workload comments provided by human operators. Secondly, high-order and two-block pilot models are identified as transfer functions from this experimental data, and the relation between these pilot models and the corresponding workload comments is analyzed. Based on the analysis, a method for estimating workload levels is proposed. Thirdly, by using H_∞ control theory, flight controller is designed to achieve fixed workload levels through the proposed method to estimate workload levels. The controller also realizes disturbance rejection and tracking performance. Finally, the effectiveness of the proposed flight controller is confirmed by demonstration experiments with the designed controller.

2 Experimental Details

2.1 Experimental Apparatus and Procedure

The experimental apparatus is depicted in Fig. 1. The display has two visual tracking positions, the follower position, y', and the target position, r. A human operator controls the stick angle, δ, in order to keep the follower centered in the moving square target throughout a 50 second time interval. The follower position, y', is a disturbed output of a controlled dynamics model whose input is δ. A block diagram of a closed-loop system, which includes a human operator, is shown in Fig. 2. In this figure, the human operator is modeled as a two-inputs and one-output system. $H_1(z)$ denotes a

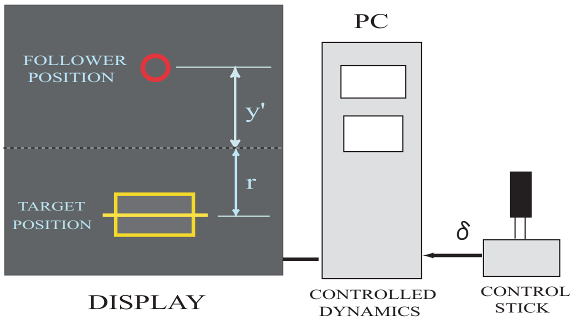

Fig. 1 Experimental apparatus

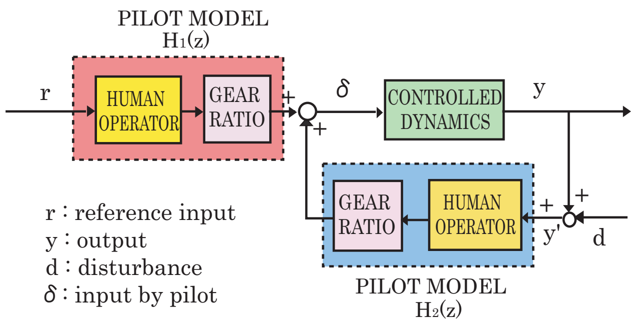

Fig. 2 Block diagram

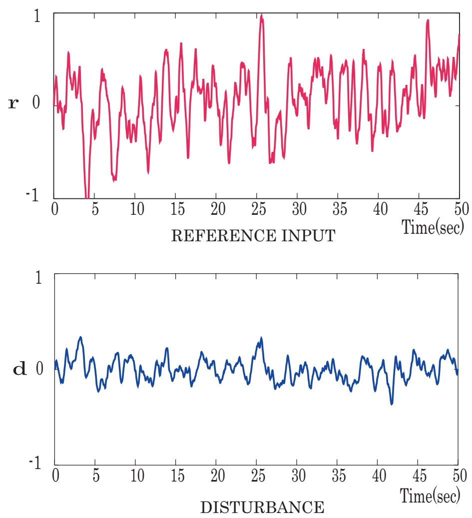

Fig. 3 Reference input and disturbance

feed-forward pilot model. It represents human operation, which senses the target position r and controls the stick angle. $H_2(z)$ denotes a feedback pilot model. It represents human operation, which senses the follower position y' and controls the stick angle. In the case of the tracking experiment, which provides two visual tracking positions for a human operator, it is assumed that the human operator has two transfer functions, $H_1(z)$ and $H_2(z)$, corresponding to these two tracking positions, respectively. Under this assumption, the pilot model is described as a two-block system consisting of $H_1(z)$ and $H_2(z)$. The gear ratio regulates the value of a human operator's input, and may be chosen arbitrarily by the human operator.

18 different types of experiments were conducted. Controlled dynamics (Table 1) were selected in order to cover various properties in terms of the natural frequency, damping ratio and the degree of dynamics. The variety of these controlled dynamics enables us to derive many characteristics of a human operator. The reference input r and the disturbance d are band-limited white noise filtered through $\omega_{nr}^2/\left(s^2+2\zeta\omega_{nr}s+\omega_{nr}^2\right)$, $\omega_{nr}=4$ (rad/sec) and $\zeta_r=1$; and $\left(0.3\times\omega_{nd}^2\right)/\left(s^2+2\zeta\omega_{nd}s+\omega_{nd}^2\right)$, $\omega_{nd}=4$ (rad/sec) and $\zeta_d=1$, respectively (Fig. 3). Compared to actual vehicle operation, the present experiments limit the task frequency. Since the inputs r and d, which simulate the actual inputs, are sufficiently random, human operators could not predict the inputs in every trial. The disturbance d was inputted in order to correctly identify H_1 and H_2. The amplitude of d was smaller than that of r, however, human operators could adequately detect the disturbance input. All the controlled dynamics are discretized with a sampling rate of 50 Hz.

Three people served as subjects I, II and III for a series of manual control experiments. They duly practiced operating under every controlled dynamics condition in order to maintain a certain level of tracking performance. This practice is necessary to identify consistent operation law through the manual control experiment so that an accurate pilot model can be obtained. The practices were repeated until identical pilot models were identified on every trial for every subject. After sufficient practice, they each selected a gear ratio. A series of manual control experiments was then carried out over 50 seconds, with data from the whole time interval captured in each trial. Only the middle 30 seconds of data were used for identification purposes since subjects could not dedicate themselves completely to stick-operation during the first and last 10 seconds of the experiments. Experimental data was

Table 1 Controlled dynamics

	ω_n	ζ	p_1	p_2	z_1	z_2
A	1	0.1				
B	5	0.8	-1			
C	5	0.1				
D	5	0.8				
E	5	0.1	-1			
F	5	0.8	-0.5			
G	10	0.4				
H	5	0.8	-5			
I	5	0.8	-3		-1	
J	5	0.8	-1+i	-1-i		
K	5	0.8	-8+8i	-8+8i		
L	5	0.8	-8+8i	-8-8i	-3+3i	-3+3i
M	5	0.8	-2+2i	-2-2i		
N	10	0.4	-3		-1	
O	10	0.8	-3		-1	
P	3	0.2	-8+8i	-8+8i	-3+3i	-3+3i
Q	2	0.8				
R	5	0.8	-3+3i	-3-3i	-5+5i	-5+5i

$$\text{A, C, D, G, Q}: \frac{\omega_n^2}{s^2+2\zeta\omega_n s+\omega_n^2}$$

$$\text{B, E, F, H}: \frac{\omega_n^2}{s^2+2\zeta\omega_n s+\omega_n^2}\times\frac{-p_1}{s-p_1}$$

$$\text{I, N, O}: \frac{\omega_n^2}{s^2+2\zeta\omega_n s+\omega_n^2}\times\frac{p_1(s-z_1)}{z_1(s-p_1)}$$

$$\text{J, K, M}: \frac{\omega_n^2}{s^2+2\zeta\omega_n s+\omega_n^2}\times\frac{p_1p_2}{(s-p_1)(s-p_2)}$$

$$\text{L, P R}: \frac{\omega_n^2}{s^2+2\zeta\omega_n s+\omega_n^2}\times\frac{p_1p_2(s-z_1)(s-z_2)}{z_1z_2(s-p_1)(s-p_2)}$$

collected together with workload evaluations provided by the human operators. Workload levels were ranked by using a 5 point rating scale. For all controlled dynamics conditions, the setting that corresponded to the most comfortable operation was defined as workload level 1, while the most wearisome one was defined as 5 in order to serve as a benchmark. The other dynamics were evaluated by comparison to these benchmark dynamics.

The pilot models were identified by a least squares method [20]. The degree of the transfer function in the pilot model is selected from 3 to 9 in order to accurately identify pilot models. Discretized pilot models are transformed into continuous forms in the following sections.

2.2 Result and Discussion

Based on the experimental results, it can be shown that subjective workload ratings correlate well with gain plots of pilot models. Researches that relate workload levels to frequency characteristics of human operations have not been applied by using experimental data. To clarify the relation between the identified pilot models and corresponding workload ratings, typical gain plots of pilot models are shown in Figs. 4, 5 and 6. What can be observed from these figures is summarized as follows.

2.2.1 *Workload level 1*

Figure 4 shows typical gain plots of pilot models which correspond to workload level 1. The gain plots of both H_1 and H_2 have constant values for low frequencies upto about 4 rad/sec, and the values decrease gently as frequency increases. In other words, it is demonstrated that human operators prefer to control the stick with constant gain values for low frequencies less than around 4 rad/sec, and disregard the reference input for frequencies above a value around 4 rad/sec. It may be noted that this characteristic is common to all subjects.

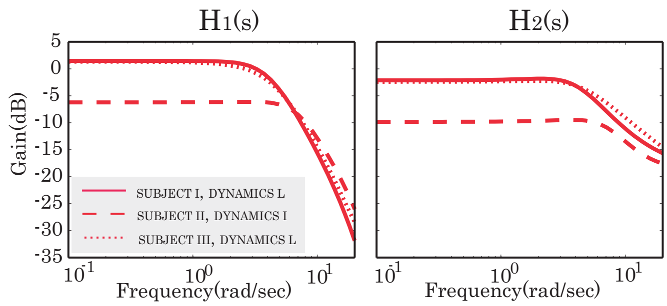

Fig. 4 Typical gain plots of workload level 1

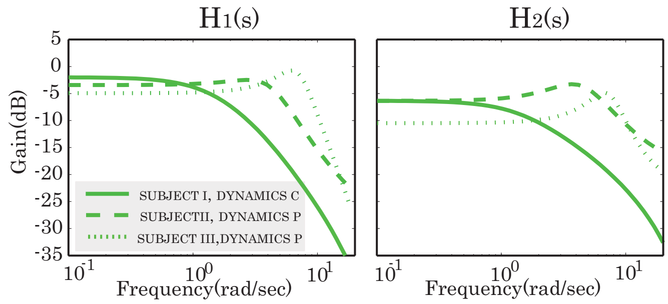

Fig. 5 Typical gain plots of workload level 3

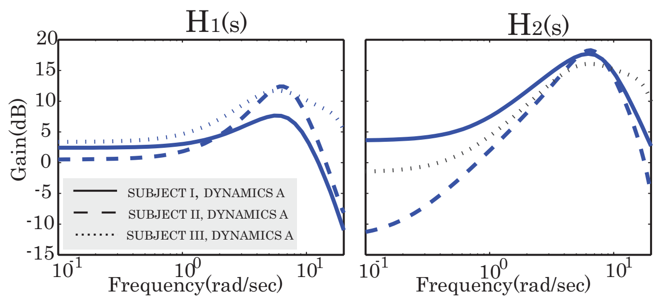

Fig. 6 Typical gain plots of workload level 5

2.2.2 *Workload level 3*

Figure 5 shows typical gain plots of pilot models which correspond to workload level 3. Comparing these plots of with Fig. 4, it is clear that gain values of both H_1 and H_2 tend to be slightly reduced for low frequencies less than 4 rad/sec or both of gain peaks appear at around 4 rad/sec. The former shows deliberate operation and the latter shows quick operation. Thus when having to cope with such a difficult operation, the human operators make an effort to achieve the desired objectives. The evaluations of workload levels provided by the human operators consequently increase.

2.2.3 Workload level 5

Figure 6 shows typical gain plots of pilot models which correspond to workload level 5. They are similar in shape to Fig. 5. It should be noted that the peak gain values of both H_1 and H_2 are significantly higher than those of Fig. 5. They represent quick operation by the human operators and these significant efforts are reflected in their workload comments.

2.2.4 Comparison of H_1 and H_2

Now, the characteristics of H_1 and H_2 are considered. The gain values of H_2 tend to be larger than those of H_1 under high frequencies, especially for workload level 5 as shown in Fig. 6. This result indicates that human operators place a special emphasis on feed-back controls under high frequencies, and the deteriorations of workload levels which occur for this case are caused by attempts to increase the gain values. In addition, since the gain values of H_1 and H_2 are nearly the same under low frequencies, it is clear that human operators combine both feed-forward controls and feed-back controls for this case. Thus the results indicate that the human operators choose between feed-forward controls and feed-back controls depending on the frequency range. To relate human operation principles with workload levels, both the characteristics of H_1 and H_2 should be considered, so that the two-block pilot models may be used for predicting human operation principles.

Human operators make efforts to control the stick in order to track the target position. The amount of effort appears to determine workload levels. The results of Fig. 4 show that there exists a set of ideal gain plots shape for pilot models, which corresponds to comfortable operation. The gap between gain plots of a given pilot model and the gain plots of the ideal pilot model as in Fig. 4 indicates the increase in the workload. Using indices that measure the difference of gain plot

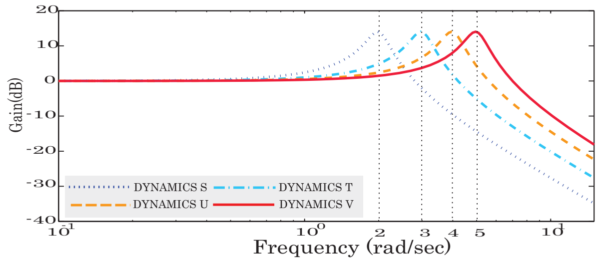

Fig. 7 Four controlled dynamics

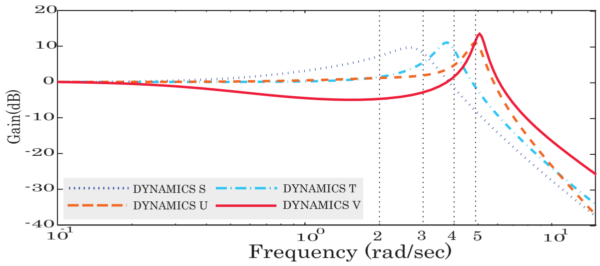

Fig. 8 Closed-loop systems (subject I)

shapes, we can mathematically estimate workload levels. In the present research, pilot models are identified as two-block models. This result shows that two-block pilot models represent each operation tendency, i.e. feed-forward, and feedback. Therefore, two-block pilot models are appropriate for the accurate analysis of human behavior related to the present two visual tracking position problems.

2.3 The Limits of Controllable Frequency

From the above discussion, it may be inferred that human operators disregard the reference input under high frequency conditions. Results indicate there is a limit frequency that corresponds to limitations in human operation. In order to obtain the limits of controllable frequency, additional experiments were carried out. Four additional types of experiments were conducted. Controlled dynamics were applied as in Table 2.

Gain plots of the controlled dynamics for the second set of experiments are shown in Fig. 7, and those for a closed-loop system, consisting of pilot models and controlled dynamics, are

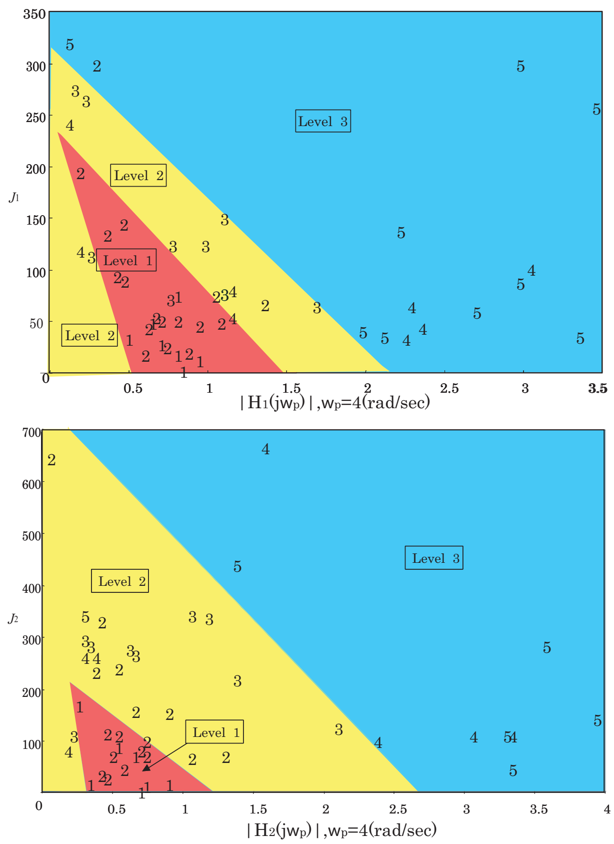

Fig. 9 Estimation indices and workload levels

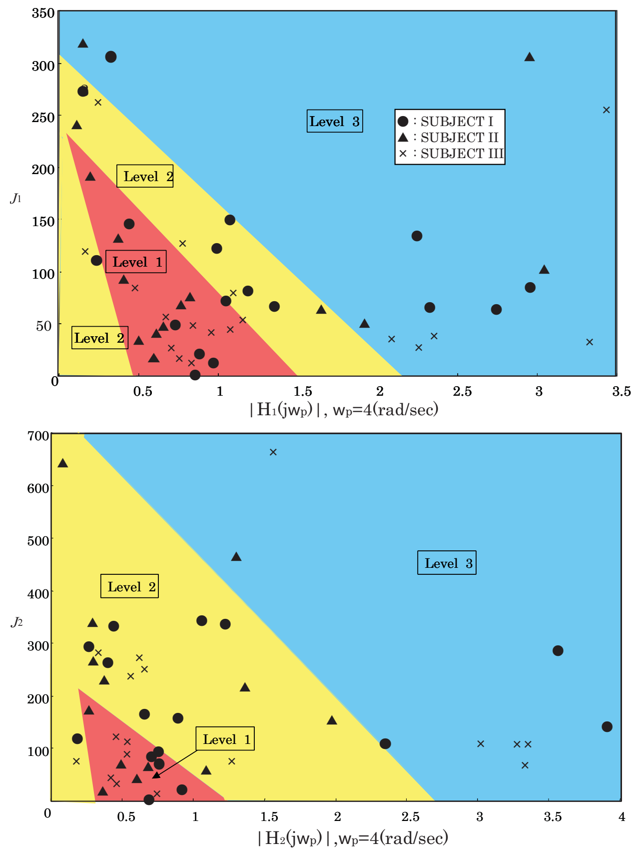

Fig. 10 Estimation indices and three subjects

shown in Fig. 8. The closed-loop systems directly indicate tracking performance. Comparing Fig. 7 with Fig. 8, the human operator acts to decrease peak values while enlarging the bandwidth of controlled dynamics whose peak frequency is less than or equal to 4 rad/sec. However, a peak value and bandwidth of controlled dynamics whose peak frequency is more than 4 rad/sec are only slightly changed. These results show that human operators cannot operate under high frequency conditions of more than 4 rad/sec. This result is common to all three subjects. Based on these experimental results, it is valid to assume that the limit of controllable frequency for the task is 4 rad/sec.

Table 2 Additional controlled dynamics

Controlled dynamics	ω_n (rad/sec)	ζ
S	2	0.1
T	3	0.1
U	4	0.1
V	5	0.1

$$S,\ T\ ,U\ ,V : \frac{\omega_n^2}{s^2+2\zeta\omega_n s+\omega_n^2}$$

3 Estimation method

3.1 Estimation Indices Based on Comfortable Model

Two types of estimation indices were established in order to objectively estimate workload levels using mathematical descriptions. In the previous section, it was said that there exists a set of ideal gain plots of pilot models that correlate well with comfortable human operations. In this paper, a pair of gain plots selected from this set was labeled as the comfortable model (CM). In the following subsections, the pilot model identified for the case when subject I controls dynamics L is adopted as a CM.

Ratings of workload levels were related to the difference in gain plot shapes between the given pilot models and a CM under a low frequency of less than 4 rad/sec, which is the observed limit of controllable frequency for human operation. To evaluate the difference, a cost index J_i is introduced as follows.

$$J_i = \int_0^{\omega_p} \left| \frac{|H_{CMi}(j\omega)|}{|H_{CMi}(j\omega_0)|} - \frac{|H_i(j\omega)|}{|Hi(j\omega_0)|} \right| d\omega \quad (1)$$

Where $i = 1,2$, $\omega_0 = 0.1$(rad/sec) and $\omega_p = 4$(rad/s). $H_{CM1}(s)$ and $H_{CM2}(s)$ are feed-forward and feed-back CMs, respectively. $H_1(s)$ and $H_2(s)$ are other pilot models.

In addition, gain values of pilot models at 4 rad/sec also affect workload levels. Since this frequency corresponds to the observed limit of human operation, human operators are subject to the most difficult task-operation at 4 rad/sec. I will accordingly also make use of the following index,

$$|H_i(j\omega_p)|, i = 1,2, \omega_p = 4\text{(rad/sec)}. \quad (2)$$

The relation between indices (1), (2) and workload levels are shown in Figs. 9 and 10. Workload levels rated by all three subjects are plotted in Fig. 9, and each subject's ratings are plotted in Fig. 10. The fields are divided into three groups: levels 1, 2 and 3.

3.2 Estimation Method

Considering which levels $H_1(s)$ and $H_2(s)$ belong to, a method to estimate workload levels is proposed (Table 3). For example, if both $H_1(s)$ and $H_2(s)$ belong to level 1, workload levels are estimated to be 1. In this way, workload levels corresponding to every pair of values for H_1 and H_2 are estimated, as displayed in Table 3. Compared with human operators perceived workload and estimated workload by the proposed method, they agree to 95 percent. Then, the effectiveness of this method is confirmed.

Table 3 Estimation method

$H_1(z)$	$H_2(z)$	Workload level
Level 1	Level 1	1
Level 1	Level 2	2
Level 2	Level 1	2
Level 2	Level 2	3
Level 2	Level 3	4
Level 3	Level 2	4
Level 3	Level 3	5

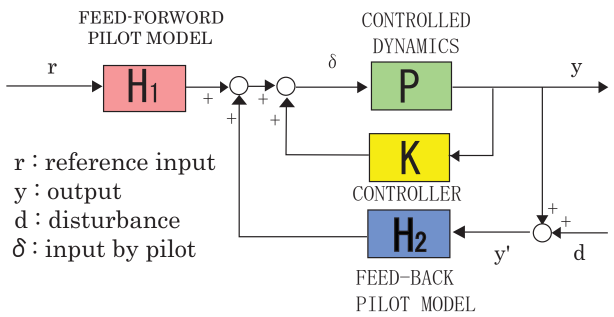

Fig. 11 Feed-back system

4 Flight Controller Design

4.1 Outline of Controller Design

This subsection outlines how that the proposed method, which estimates workload levels through pilot models, enable us to design controller on assumed workload levels.

There is a feed-back system including the dynamics of pilots and flight controller (Fig. 11). Tracking performance and disturbance rejection are respectively represented as the transfer functions from r to y and d to y including pilot models. As may be observed from the experimental results, it is considered that human operators make effort to adjust the gain values of these transfer functions at certain characteristics described in the next subsection (see Figs. 12 and 14). On account of designing flight controller which assists human operation, firstly, the ideal pilot models correlated to workload level 1, which is evaluated using the proposed estimation method are chosen. Secondly, the controller

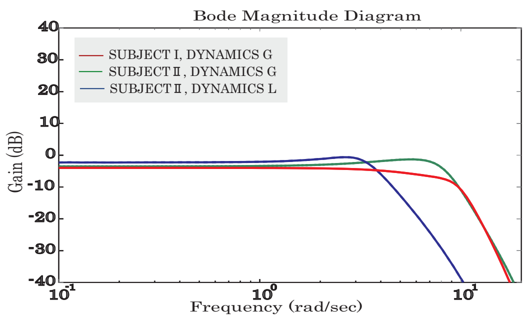

Fig. 12 Ideal gain plots of tracking performance

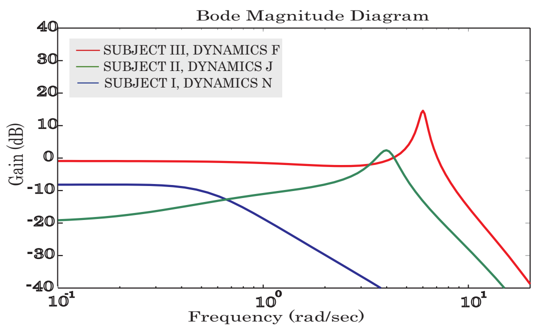

Fig. 13 Undesirable gain plots of tracking performance

is designed in order that two transfer functions which show tracking performance and disturbance rejection attain the desired characteristics. The two transfer functions consist of the chosen pilot models and controlled dynamics. Then the designed flight controller guarantees comfortable human operations. There are many ways of human operation which attain the desired characteristics. However, the designed controller do not impose larger levels of workload than the assumed levels of workload because it can be rationally presumed that the human operator chooses the most comfortable operation as far as the task is attained.

4.2 Design Conditions

This paper aims to design flight controller which ensure workload level 1 and both ideal characteristics of tracking performance and disturbance rejection.

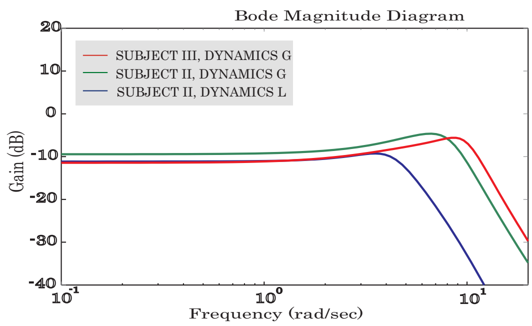

Fig. 14 Ideal gain plots of disturbance rejection

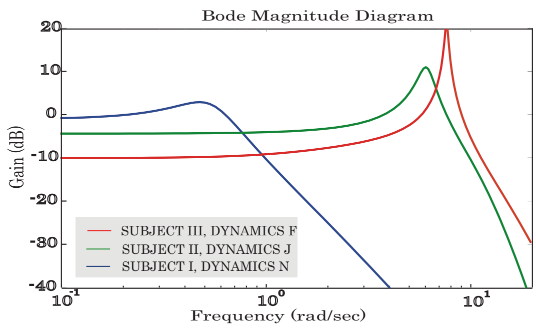

Fig. 15 Undesirable gain plots of tracking performance

4.2.1 Tracking Performance

The transfer function from reference input r to output y shows tracking performance. As may be observed from the experimental results, Fig. 12 shows ideal gain plots of tracking performance, and Fig. 13 shows undesirable gain plots of tracking performance. Compared with Fig. 12 and Fig. 13, design conditions to the gain plots of transfer function from r to y are proposed as follows.

- Design Condition 1
  The droop, which means a drop in gain value from 0dB, becomes more than -5dB for low frequencies upto about 4 rad/sec.

- Design Condition 2
  The peak value of gain is less than 0dB.

4.2.2 Disturbance Rejection

The transfer function from disturbance input d to output y shows disturbance rejection. As may be observed from the experimental results, Fig. 14 shows ideal gain plots of disturbance rejection, and Fig. 15 shows undesirable gain plots of disturbance rejection. Compared with Fig. 14 and Fig. 15, design conditions to the gain plots of transfer function from d to y are proposed as follows.

- Design Condition 3
  The peak value of gain is less than -5dB.

Pilot models which correspond to workload level 1 are chosen through the proposed method, and then flight controller is designed in order that the two transfer functions, which is from r to y and d to y consisting of the chosen pilot models, attain the above 3 conditions. By using H_∞ loop shaping technique[21], flight controller is designed which satisfy above 3 conditions.

4.3 Demonstration Experiment

In order to confirm the effectiveness of the designed controller, demonstration experiment was carried out with respect to controlled dynamics A (see Table 1):one with controller and another without controller. As a result, workload rating is subjectively evaluated as 5 without controller, but then workload rating is subjectively evaluated as 1 with the designed controller. Fig. 16 shows gain plots of pilot models. By using the proposed method of workload estimation, the pilot model which corresponds to controlled dynamics with the controller is evaluated as workload level 1. Fig. 17 and 18 respectively show the gain plots of the tracking performance and the disturbance rejection. With the designed controller, both of them satisfy the design conditions. From above discussion, it is demonstrated that the designed controller ensures workload level 1 and desired characteristics of both tracking performance and disturbance rejection.

5 Conclusion

In this paper, the new method to estimate workload levels was proposed, and a flight controller was designed to assist pilot operation through the proposed method. A series of manual control experiments which mimic the control of longitudinal dynamics of aircraft was carried out, and pilot models were identified as high-order and two-block transfer functions from the resultant experimental data. There exists a set of ideal gain plots of pilot models that correlate well with comfortable human operations, and one ideal model was defined as a comfortable model. Based on a pair of ideal gain plots, two types of indices have been established to measure the gap between given pilot models and the pair of ideal gain plots. These indices clearly represent that workload levels depend on operation principles of human operators. Based on these indices, the new method,

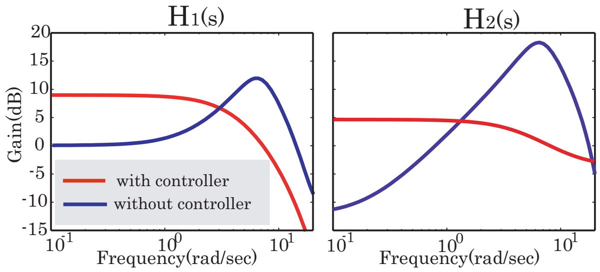

Fig. 16 Comparison of pilot model

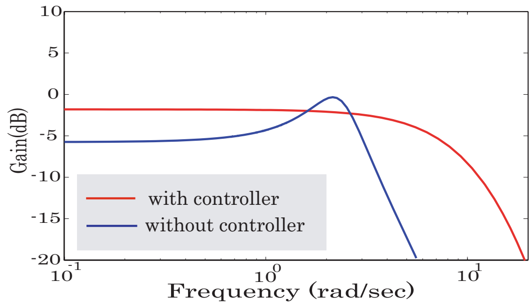

Fig. 17 Comparison of tracking performance

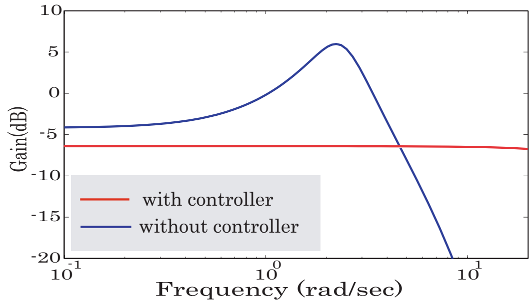

Fig. 18 Comparison of disturbance rejection

which mathematically and objectively estimates workload levels, has been proposed. The frequency characteristics of the pilot models enable us to design flight controller that ensure human-friendly operation. Demonstration experiments show the effectiveness of the designed controller.

This study has limited the task to the frequency of operations. The task influences pilot performance, so further research on the relationship between human behavior and task type is necessary. Although operation principles depend on types of tasks, if the desired closed-loop characteristics and the comfortable pilot model are investigated, human-friendly control systems can be designed. This research analyze human operation for low frequencies less than around 4 rad/sec. In the future, high-frequency content of human behavior should be analyzed to design man-machine systems.

References

[1] C. D. Wickens. *Engineering psychology and human performance.* 2nd ed, New York:Harper Collins, 1992, pp. 389-402.

[2] S. S. Mulgund and G. L. Zacharias. A situation-driven adaptive pilot/vehicle interface. *Proc. the 1996 IEEE Human Interaction with Complex Systems Symposium*, 1996, pp. 193-198.

[3] Y. Kuriyagawara and I. Kageyama. A modeling of heart rate variability to estimate mental work load. *SMC99(IEEE)*, ISBN0-7803-5734-5, Oct.1999(Tokyo, Japan), pp. II294-299.

[4] T. P. Neal and R. E .Smith. An in-flight investigation to develop control system design criteria for fighter airplanes. *U.S. Air force Flight Dynamics Laboratory report AFFDL-TR-70-74*, 1970, VOLUME1.

[5] G. E .Cooper and R. P .Harper, Jr.. The use of pilot rating in the evaluation of aircraft handling qualities. *NASA TND-5153*, 1969.

[6] P. A. Hancock and M. H. Chignell. Mental workload dynamics in adaptive interface design. *IEEE trans. SMC*, 1988, pp. 647-658.

[7] P. A. Hancock and J. K. Caird. Experimental evaluation of a model of mental workload. *HUMAN FACTORS*, 1993, 35(3), pp. 413-429.

[8] R. W. Roigo. A comparison between human operator and optimum linear controller RMS-error performance. *IEEE trans. HFE*, 1962, pp. 18-22.

[9] A. Skolnick. Stability and performance of manned control systems. *IEEE trans. HFE*, 1966, pp. 115-124.

[10] R. G. Costello. The surge model of the well-trained human operator in simple manual control. *IEEE trans. MMS*, 1968, pp. 2-9.

[11] R. C. Wingrove. Measurement of pilot describing functions from flight test data with an example from Gemini X. *IEEE trans. MMS*, 1968, pp. 49-55.

[12] G. A. Jackson. A method for the direct measurement of crossover model parameters. *IEEE trans. MMS*, 1969, pp. 27-33.

[13] A. V. Phatak and G. A. Bekey. Model of the adaptive behavior of the human operator in response to a sudden change in the control situation. *IEEE trans. MMS*, 1969, pp. 73-80.

[14] M. Sadoff and C. B. Dolkas. Acceleration stress effects on pilot performance and dynamic response. *IEEE trans. HFE*, 1967, pp. 103-11.

[15] E. P. Todosiev, R. E. Rose and L. G. Summers. Human performance in single and two-axis tracking systems. *IEEE trans. HFE*, 1967, pp. 125-129.

[16] W. W. Wierwille, G. A. Gagne and J. R. Knight. An experimental study of human operator models and closed-loop analysis methods for high-speed automobile driving. *IEEE trans. HFE*, 1967, pp. 187-201.

[17] E. P. Todosiev. Human performance in a cross-coupled tracking system. *IEEE trans. HFE*, 1967, pp. 210-217.

[18] J. H. Herzog. Manual control using the matched manipulator control technique. *IEEE trans. MMS*, 1968, pp. 56-60.

[19] D. T. Mcruer and H. R. Jex. A review of quasi-linear pilot models. *IEEE trans. HFE*, 1967, pp. 231-249.

[20] N. Goto and K. Washizu. On the dynamics of human pilots in marginally controllable systems. *AIAA Journal*, 1973, pp. 310-315.

[21] P. Gahinet and P. Apkarian. A linear matrix inequality approach to H_∞ control. *International Journal of Robust and Nonlinear Control*, Vol.4, pp.421-448, 1994.